Dynamics of β_2-Adrenergic Receptor−Ligand Complexes on Living Cells[†]

Oliver Hegener,[‡,§] Lars Prenner,[§,||] Frank Runkel,[⊥] Stephan Leonhardt Baader,[@] Joachim Kappler,[||] and Hanns Häberlein*[,||]

Department of Pharmaceutical Biology, Philipps University, Deutschhausstrasse 17A, 35032 Marburg, Germany, Institute of Physiological Chemistry, Rheinische Friedrich-Wilhelm University, Nussallee 11, 53115 Bonn, Germany, University of Applied Science, Wiesenstrasse 14, 35390 Giessen, Germany, and Institute of Anatomy and Cell Biology, Rheinische Friedrich-Wilhelm University, Nussallee 10, 53115 Bonn, Germany

Received October 29, 2003; Revised Manuscript Received March 22, 2004

ABSTRACT: The agonist-induced dynamic regulation of the β_2-adrenergic receptor (β_2-AR) on living cells was examined by means of fluorescence correlation spectroscopy (FCS) using a fluorescence-labeled arterenol derivative (Alexa-NA) in hippocampal neurons and in alveolar epithelial type II cell line A549. Alexa-NA specifically bound to the β_2-AR of neurons with a K_D value of 1.29 ± 0.31 nM and of A549 cells with a K_D of 5.98 ± 1.62 nM. The receptor density equaled 4.5 ± 0.9 μm^{-2} in neurons (ρ_N) and 19.9 ± 2.0 μm^{-2} in A549 cells (ρ_{A549}). Kinetic experiments revealed comparable on-rate constants in both cell types ($k_{on} = 0.49 \pm 0.03$ s^{-1} nM^{-1} in neurons and $k_{on} = 0.12 \pm 0.02$ s^{-1} nM^{-1} in A549 cells). In addition to the free ligand diffusing with a D_{free} of $(2.11 \pm 0.04) \times 10^{-6}$ cm^2/s, in both cell types receptor−ligand complexes with two distinct diffusion coefficients, D_{bound1} (fast lateral mobility) and D_{bound2} (hindered mobility), were observed [$D_{bound1} = (5.23 \pm 0.64) \times 10^{-8}$ cm^2/s and $D_{bound2} = (6.05 \pm 0.23) \times 10^{-10}$ cm^2/s for neurons, and $D_{bound1} = (2.88 \pm 1.72) \times 10^{-8}$ cm^2/s and $D_{bound2} = (1.01 \pm 0.46) \times 10^{-9}$ cm^2/s for A549 cells]. Fast lateral mobility of the receptor−ligand complex was detected immediately after addition of the ligand, whereas hindered mobility (D_{bound2}) was observed after a delay of 5 min in neurons (up to 38% of total binding) and of 15−20 min in A549 cells (up to 40% of total binding). Thus, the receptor−ligand complexes with low mobility were formed during receptor regulation. Consistently, stimulation of receptor internalization using the adenylate cyclase activator forskolin shifted the ratio of receptor−ligand complexes toward D_{bound2}. Intracellular FCS measurements and immunocytochemical studies confirmed the appearance of endocytosed receptor−ligand complexes in the cytoplasm subjacent to the plasma membrane after stimulation with the agonist terbutaline (1 μM). This regulatory receptor internalization was blocked after preincubation with propranolol and with a cholesterol-complexing saponin α-hederin.

The β_2-adrenergic receptors (β_2-ARs)[1] mediate a variety of effects in noncardial tissues, including the relaxation of smooth muscle in blood vessels, bronchus, intestine, and uterus. They mediate glycogenolysis and glucogenesis in liver and regulate cell metabolism in skeletal muscle. The β_2-ARs are also located presynaptically in nerves where they facilitate neurotransmitter release and in brain where they regulate a variety of physiological processes. The β_2-AR belongs to the family of G-protein-coupled receptors and is subjected to a reduction in receptor sensitivity, which is called desensitization, upon short-term interaction with a specific agonist (*1*−*3*). Prolonged interactions with the β_2-AR lead to an endosomal uptake of receptor−ligand complexes; i.e., receptor proteins are internalized, thereby leading to a compensatory reduction (sequestration) of receptors in the cell membrane. In this way, the cell is able to adapt on a medium- to long-term basis to changing influences. Desensitization and sequestration of β_2-AR are finely regulated by various mechanisms involving PKA, GRK2, β-arrestin, and dynamin. These processes are crucially important to numerous physiological and pathophysiological mechanisms (*4*). Receptor downregulation is a major limiting factor for the medication of chronic obstructive diseases of the respiratory tract, and is additionally discussed in connection with the development of the dependence that is triggered by alcohol and drugs with action on the central nervous system (*5*). On the other hand, the specific influence on the β_2-AR density is relevant to the treatment of certain pathophysiological conditions. For example, the increased level of expression of the β_2-AR through the inhalational administration of corticosteroids in the lung is used to maintain the

[†] This work was financially supported by Engelhard Arzneimittel (Niederdorfelden, Germany).

* To whom correspondence should be addressed: Institute of Physiological Chemistry, Rheinische Friedrich-Wilhelm University, Nussallee 11, D-53115 Bonn, Germany. E-mail: haeberlein@institut.physiochem.uni-bonn.de. Phone: +49 228 736555. Fax: +49 228 732416.

[‡] Philipps University.

[§] These authors contributed equally to this work.

[||] Institute of Physiological Chemistry, Rheinische Friedrich-Wilhelm University.

[⊥] University of Applied Science.

[@] Institute of Anatomy and Cell Biology, Rheinische Friedrich-Wilhelm University.

[1] Abbreviations: β_2-AR, β_2-adrenergic receptor; FCS, fluorescence correlation spectroscopy; Alexa-NA, Alexa Fluor 532−arterenol species; PKA, protein kinase A; GRK2, β-adrenergic receptor kinase.

10.1021/bi035928t CCC: $27.50
Published on Web 05/01/2004

responsiveness of the alveolar epithelium and the smooth muscles of the respiratory tract during long-term sympathomimetic medication (*6*). The classical biochemical investigation of receptor−ligand interactions, which is based on radioreceptor binding studies on membrane preparations, however, does not represent these regulatory processes. Therefore, the direct observation of the interaction of ligands with their receptors on living cells and the influence of various drugs on such systems would be of great importance. Fluorescence correlation spectroscopy (FCS) is a technique for investigating adaptive processes on living cells at the molecular level with minimal disturbance of the cells that are being investigated, if suitable fluorescent probes for these processes are available (*7*). FCS measures the diffusion times of individual molecules by detecting fluctuations in fluorescence intensity (*8*−*10*). Changes in the diffusion characteristics of fluorescence-labeled probes therefore allow conclusions to be drawn about different functional states, such as those occurring during signal transduction or subsequent regulation of receptor−ligand complexes. Recently, in FCS experiments, a concentration-dependent increase in the level of specific binding of a dye-labeled muscimol derivative was demonstrated by the positive cooperative activity of a co-incubated benzodiazepine, which was selectively found in $GABA_A$ receptor−ligand complexes with hindered lateral mobility (*11*).

Here, we describe the synthesis of a dye-labeled arterenol derivative based on the dependence of the β-adrenergic ligand subtype selectivity on catecholamine substitution at the amine function. To create a more β_2-specific ligand from β_1-preferring arterenol, the succinimidyl ester-activated fluorescent dye Alexa 532 was introduced at this position via nucleophile substitution. Using the FCS technique, we describe β_2-adrenergic receptor−ligand interactions, the varying lateral receptor mobility following ligand binding, and the internalization of receptor−ligand complexes using hippocampal neurons and alveolar epithelial type II cells.

MATERIALS AND METHODS

Synthesis of the Alexa−Arterenol Species. Two milligrams of arterenol (11.83 μM) (Sigma-Aldrich, Taufkirchen, Germany) and 1.0 mg of Alexa Fluor 532 carboxylic acid, succinimidyl ester 6-isomer (1.38 μM) (Molecular Probes, Leiden, The Netherlands), were dissolved separately in 0.5 mL of ethanol (99.5%) (Merck, Darmstadt, Germany). The solutions were combined dropwise and stirred for 24 h. The reaction mixtures were purified by high-performance liquid chromatography (HPLC) using a LiChrospher RP8-select B (125 mm × 4 mm, 5 μm) column (Merck). The eluent was a mixture of acetonitrile (23.0%), H_2O (72.5%), methanol (4.0%), and 85% H_3PO_4 (0.5%), with a flow rate of 0.9 mL/min; all solvents were HPLC grade (Merck). Water was taken from a Millipore Milli-Q System (Millipore GmbH, Eschborn, Germany). Peak detection was at 254 nm parallel to 514 nm. The resulting yield was 0.9 mg (1.15 μM, 83%). The purity of the product was >99%, proven by HPLC. The identity of the product was confirmed by high-resolution mass spectrometry [AutoSpec mass spectrometer (Waters, Milford, MA), methanol as the solvent, and a flow rate of 10 μL/min] for Alexa-NA (measured value of 778.8823, calcd 778.8840).

Cell Culture. The hippocampal neurons were prepared from brains of Sprague-Dawley rat embryos at embryonic day 18 by microdissection (*12*). The cells were triturated and seeded at a density of approximately 2.5×10^5 to 18 mm poly-L-lysine (Sigma)-coated glass coverslips in 12-well plates (Nunc, Wiesbaden, Germany). After being cultured for 8 days in 5% CO_2 at 37 °C using Start-V medium (Biochrome, Berlin, Germany), cells were used for experiments from day 9 to 14.

The A549 human cancer cell line was obtained from the U.S. National Cancer Institute (NCI, Bethesda, MD) and was used for passages 190−210. The cells were maintained in RPMI 1640 with glutamine and 10% fetal calf serum (both from Gibco BRL, Karlsruhe, Germany). For the FCS experiments, the cells were seeded at a density of 2.5×10^5 cells/cm^2 to 18 mm poly-L-lysine-coated glass coverslips and cultured in 12-well plates (Nunc) for 2−3 days to 80% confluency and used for experiments from day 4 to 7.

Receptor Binding Studies. Prior to the FCS experiments, the cells were washed three times with Locke's solution [5 mM HEPES, 154 mM NaCl, 5.6 mM KCl, 1 mM $MgCl_2$, 3.6 mM Na_2CO_3, 20 mM glucose, and 2.3 mM $CaCl_2$ (pH 7.4)] at 37 °C. The coverslips were mounted on a coverslip carrier with an incubation volume of 300 μL. For the binding studies, the cells were incubated for 15 min with different concentrations of Alexa-NA (from 0.1 to 240 nM for saturation experiments, 5 nM for determination of k_{on}) in Locke's solution at 20 °C. For every data point, at least 10 single measurements of 30 s runs were performed on three to four cells from two different cell preparations. To determine the level of nonspecific binding, cells were preincubated with 5 μM competitor (terbutaline hemisulfate, propranolol HCl) for 1 h followed by a second incubation with 5 nM Alexa-NA. A negative control was performed by incubating the cells with 5 nM Alexa Fluor 532 carboxylic acid, succinimidyl ester 6-isomer.

Receptor Regulation. For the time-dependent detection of the regulatory processes, hippocampal neurons and A549 cells were initially incubated with 5 nM Alexa-NA. Data were collected every minute in 30 s measurements. The data points represent the average of two sequential 30 s runs on single cells. Experiments were performed in duplicate.

Cell scans of A549 cells were performed in the *z*-direction initially and after a 5, 20, 30, and 60 min incubation period with 10 nM Alexa-NA. Stimulation of the β_2-AR internalization was induced by co-incubation with 1 μM terbutaline. To inhibit the internalization process, A549 cells were preincubated with 1 μM α-hederin for 24 h at 37 °C in 5% CO_2 and washed three time with PBS (pH 7.4) at 20 °C.

FCS Setup. FCS measurements were performed with confocal illumination of a 0.19 fL volume element in a ConfoCor instrument (Zeiss, Jena, Germany). For excitation, the 514 nm line of an argon laser (LGK 7812 ML 2, Lasos, Jena, Germany) was focused through a water immersion objective (C-Apochromat, 63×, NA 1.2, Zeiss) into the sample [power density in the focal plane, measured before the objective (p_{514}), of 14.2−109 kW/cm^2]. The emitted fluorescence was separated from the excitation light with a dichroic filter and a band-pass filter. The intensity fluctuations were detected by an avalanche single-photon counting module (SPCM-AQ Series, EG&G Optoelectronics Canada Inc., Vaudreuil, PQ). The signal was correlated online to data

acquisition with a digital hardware correlator (ALV-5000, ALV, Langen, Germany).

Focus positioning to the upper membrane of the cell soma was done both by visual inspection in the *x*- and *y*-directions and by motor-aided scanning of the autofluorescence of the cell in the *z*-direction. Taking the position of the half-maximal autofluorescence of the upper membrane, the focus took in fast-diffusing free molecules and slow-diffusing ligands bound to a kind of receptor as well. Furthermore, the lower part of the focus was localized in the cytoplasm just below the plasma membrane, allowing the detection of internalized ligands.

Cell scans were performed by moving the focus in the *z*-direction through the cell to characterize the initial autofluorescence of the cell and the fluorescence intensity after ligand incubation. The cell scan showed a two-peak profile for the lower and upper membrane. The range between the two peaks characterized the fluorescence intensity of the cytoplasm, which was integrated for quantification.

Data Analysis. In a three-dimensional Gaussian volume, the autocorrelation function $G(\tau)$ for j different diffusing components is given by the following equation (*13*):

$$G(\tau) = 1 + \frac{\sum_{j=1}^{n} Q_j^2 N_j}{(\sum_{j=1}^{n} Q_j N_j)^2} \frac{1}{1 + \tau/\tau_{Dj}} \sqrt{\frac{1}{1 + (\omega_0/z_0)^2 \tau/\tau_{D_j}}} \quad (1)$$

with

$$\tau_{D_j} = \frac{{\omega_0}^2}{4D_j} \quad (2)$$

and

$$Q_j = \sigma_j \eta_j g_j \quad (3)$$

where N_j is the average number of molecules of species j in the volume element, τ_{D_j} the diffusion time constant of species j, ω_0 the radius of the observation volume in the focal plane, z_0 the radius of the observation volume in the z-direction, D_j the translational diffusion coefficient of species j, Q_j the quantum yield factor, σ_j the absorption cross section, η_j the fluorescence quantum yield, and g_j the fluorescence detection efficiency of species j.

When all fluorescent components j have the same count rate per molecule (i.e., all Q_j values are the same) and diffuse on a cell surface, then eq 1 simplifies to

$$G(\tau) = 1 + \frac{1}{N} \times \sum_{j=1}^{n} \frac{y_j}{1 + \tau/\tau_{D_j}} \quad (4)$$

where y_j is the fraction of species j to the autocorrelation amplitude, τ_{D_j} the diffusion time constant of species j, and N the total number of molecules in the detection volume element.

It is known that association and dissociation of the receptor−ligand complex may have an influence on the diffusion time constants (*14*, *15*). Although a model that takes into account these processes would be more relevant, simplifications in eq 4 are suitable for calculating averaged diffusion time constants for freely diffusing ligands and for receptor−ligand complexes with free and hindered lateral mobilities which change by more than 1 order of magnitude.

Prior to the experiments, the volume element of observation was calibrated. For this purpose, a defined concentration of rhodamine 6G was added to the extracellular solution and the autocorrelation function for the dye diffusion was recorded. The radii ω_0 and z_0 were calculated (according to eqs 1 and 2) from the determined diffusion time constant for rhodamine 6G and a diffusion coefficient of 280 $\mu m^2/s$ (*16*).

Immunocytochemical Detection of the β_2-AR. A549 cells were cultured, as described previously, and incubated after 4 days in culture on glass coverslips. Treatment of the cells with 10 μM terbutaline hemisulfate (Sigma) for 10 min, 10 μM propranolol HCl (Sigma) for 1 h, and 1 μM α-hederin (Sigma) for 24 h was performed at 37 °C in 5% CO_2. Cells were fixed with 4% paraformaldehyde for 10 min. Permeabilization of the cells was performed with 0.2% Triton X-100 in PBS for 5 min at room temperature. Nonspecific anti-β_2 antibody binding was blocked with 3% bovine serum albumin in PBS buffer (pH 7.4) and 0.2% Triton X-100 for 1 h at room temperature. To detect the β_2-AR on A549 cells, the combination of anti-β_2 antibody H20 (1:240 dilution, incubation for 1 h at room temperature; Santa Cruz Biotechnologies, Santa Cruz, CA) and Alexa 488-labeled goat anti-rabbit antibody (1:500 dilution, incubation for 1 h at room temperature; Molecular Probes, Leuven, The Netherlands) was used. Cells were visualized by staining F actin with phalloidin-TRITC (Sigma) [stock solution of 100 μg/mL DMSO; staining with a stock solution diluted 1:1000 with 0.2% Triton X-100 in PBS (pH 7.4)] for 5 min at room temperature. Cells were washed with 0.2% Triton X-100 in PBS (pH 7.4) at 20 °C thrice after every step.

Cultured A549 cells were examined with a Leica TCS SP2 confocal laser scanning unit equipped with an argon and a HeNe laser. The laser scanning module was attached to the DM IRE 2 inverse microscope. Images were recorded and processed with the Leica LCS software. A 40× objective (1.25 numerical aperture) was used throughout the experimental design. To ensure equal illumination for all treatments, the same laser intensity, acousto-optical tunable filter settings, and signal amplification settings were applied. Images were recorded at a resolution of 512 × 512 pixels. The pinhole was set to 1 Airy (82 μm).

RESULTS

FCS binding studies were first performed with the Alexa 532−arterenol species (Alexa-NA) on pyramidal hippocampal neurons of the rat which express the β_2-adrenergic receptor (β_2-AR) on the cell soma (*17*, *18*) and which exhibited low cellular autofluorescence. These primary neurons showed a maximum, noncorrelatable fluorescence intensity in the biomembrane of approximately 2.5 kHz with a prevailing laser excitation energy of 14.2 kW/cm^2. This very low background signal was an essential prerequisite for conducting subsequent binding studies using ligand concentrations in the nanomolar range.

When arterenol (noradrenaline, NA) was labeled with the fluorescent dye Alexa 532 at the primary amine moiety to

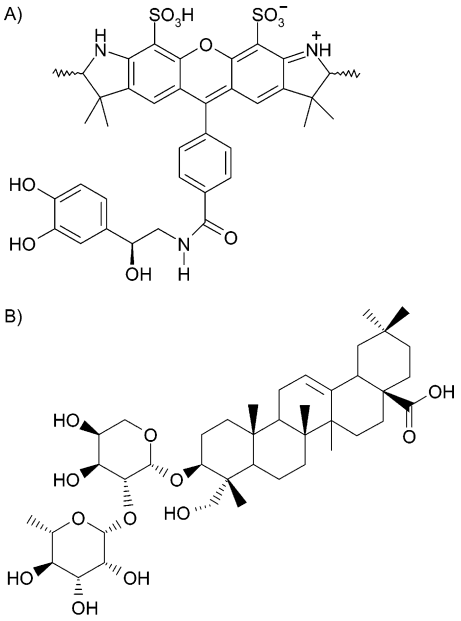

FIGURE 1: Chemical structures of Alexa-NA (A) and α-hederin (B).

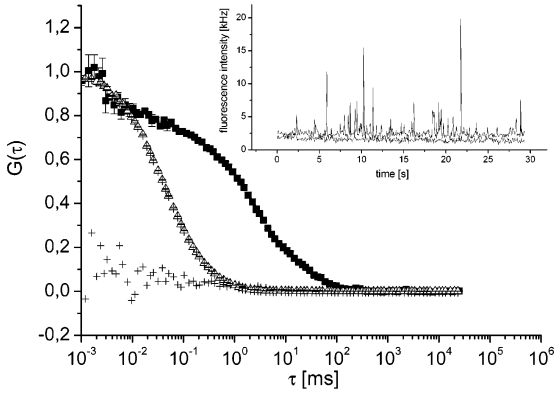

FIGURE 2: Normalized autocorrelation curves: (△) freely diffusing Alexa-NA with a τ_{free} of 45.5 ± 0.89 μs (n = 20) above the cells, (■) Alexa-NA bound to the cell membrane of a hippocampal neuron with a τ_{bound1} of 1.84 ± 0.17 ms (n = 20) and a τ_{bound2} of 158.6 ± 40.4 ms (n = 20), and (+) autofluorescence of the nonincubated neuronal membrane. The inset shows the fluorescence trace of the incubation with 1 nM Alexa-NA in comparison with the nonincubated membrane of a hippocampal neuron.

obtain a β_2-AR ligand according to the general structure−binding relationship of adrenergic ligands (*19*), the reaction product termed Alexa-NA was obtained with a high yield (83%) and purity (>99%) after HPLC purification (Figure 1). The identity of the product was confirmed by high-resolution mass spectrometry for Alexa-NA (measured value of 778.8823, calcd 778.8840). After incubation of hippocampal neurons with 1 nM Alexa-NA, fluorescence correlation spectroscopy (FCS) revealed an increase in the fluorescence intensity at the neuronal plasma membrane, which exceeded the background approximately 10-fold in the form of autocorrelating signals, amounting to approximately 20 kHz (Figure 2, inset). In FCS binding studies, bound and freely diffusing ligands are differentiated by their characteristic diffusion time constants, while the corresponding fluorescence intensities are measured for quantification. The evaluation of the FCS autocorrelation curves yielded for Alexa-NA in Locke's solution a diffusion time constant (τ_{free}) of 45.5 ± 0.89 μs (n = 20), from which a diffusion coefficient (D_{free}) of (2.11 ± 0.04) × 10^{-6} cm^2/s was calculated (Figure 2). In equilibrium, Alexa-NA showed saturable binding to the β_2-AR with a dissociation constant (K_D) of 1.29 ± 0.31 nM (n = 2) (Figure 3A) and a maximum number of binding sites (B_{max}) of 5.96 ± 0.27 nM (n = 2), corresponding to a receptor density (ρ) of 4.5 ± 0.9 μm^{-2} (n = 6) on the cell bodies. Competition experiments with a 1000-fold excess of the β_1/β_2-specific competitor propranolol (β_1/β_2-agonist) yielded a level of nonspecific binding of 23%. However, competition of the Alexa-NA binding with increasing concentrations of nonlabeled arterenol yielded an IC_{50} value of 7.09 ± 0.51 μM (n = 3), from which an inhibition constant (k_i) of 3.86 ± 0.28 μM (n = 3) was calculated which was 1000-fold higher than the K_D of Alexa-NA. An additional inhibition experiment with a 1000-fold excess of the β_2-specific agonist terbutaline resulted in a level of nonspecific binding of 25%, similar to that observed with propranolol. It could thus be concluded that the coupling of the dye to the amine function of arterenol increased the affinity for the β_2-AR as expected from the structure−binding relationship of adrenergic ligands (*19*). A negative control of pure dye incubated with the cells revealed no membrane-related fluorescence in the FCS experiment. Only freely diffusing dye molecules were present.

Interestingly, the autocorrelation curve obtained from binding experiments on the neurons reproducibly revealed two distinct diffusion time constants for the bound ligand [τ_{bound1} = 1.84 ± 0.17 ms (n = 20) and τ_{bound2} = 158.6 ± 40.4 ms (n = 20)], indicating the existence of two subpopulations of receptor−ligand complexes with different mobilities [D_{bound1} = (5.23 ± 0.64) × 10^{-8} cm^2/s and D_{bound2} = (6.05 ± 0.23) × 10^{-10} cm^2/s] (Figure 2).

When the kinetics of the bound states were followed in a time-dependent binding experiment involving 5 nM Alexa-NA on hippocampal neurons (Figure 3B), an overall binding rate constant (K_{on}) of 0.49 ± 0.03 s^{-1} nM^{-1} (n = 2) was measured. Moreover, a time-dependent evaluation of the different diffusion time constants revealed a binding curve for the receptor−ligand complex with τ_{bound1}, which corresponded to a one-site binding model, whereas the part of the free ligand with τ_{free} dropped simultaneously (Figure 4A). Remarkably, the formation of receptor−ligand complexes with low mobility (τ_{bound2}) occurred later and was a transient event. The maximum value of 38% for τ_{bound2} was reached after 5 min, and slowly dropped again thereafter, suggesting that the low-mobility complexes are formed from high-mobility complexes (τ_{bound1}) (Figure 4A).

To determine the subcellular localization of bound ligands, neurons were scanned by moving the laser focus along the z-direction through the cell. Analysis at various points in time revealed an increase in the fluorescence intensity in the neuronal plasma membrane upon the appearance of τ_{bound1}. Intensive fluorescence tracks for individual intracellular events correlated with the appearance of the receptor−ligand complex with τ_{bound2} (Figure 5). Taken together, these data clearly demonstrate heterogeneity of β_2-AR states in hippocampal neurons and indicate that the lower receptor mobility corresponds to a state related to up- and down-regulation processes.

To further elaborate on these findings and to evaluate the cell type dependence of the binding of Alexa-NA to the β_2-

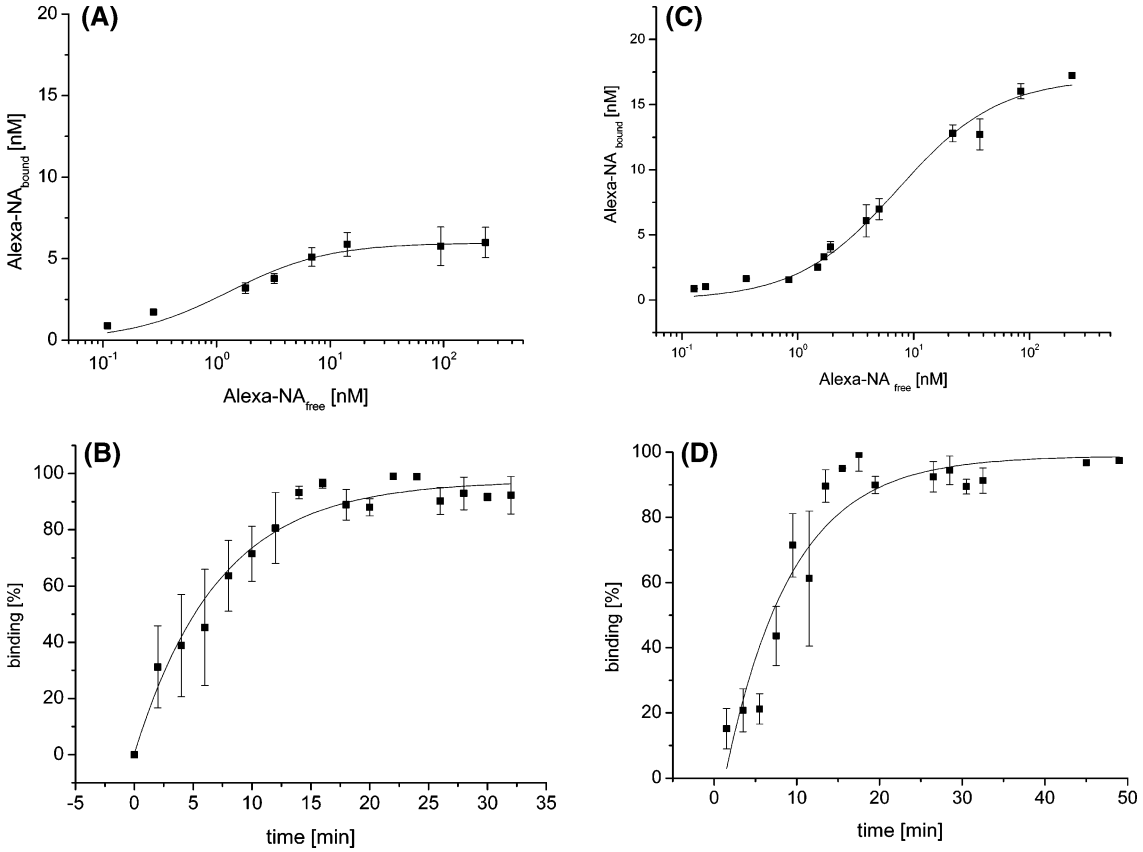

FIGURE 3: Comparison of binding of Alexa-NA to hippocampal neurons and A549 cells. (A) Saturation of binding of Alexa-NA to hippocampal neurons ($n = 2$). (B) Time-dependent binding of 5.0 nM Alexa-NA to hippocampal neurons ($n = 2$). (C) Saturation of binding of Alexa-NA to A549 cells ($n = 2$). (D) Time-dependent binding of 6.8 nM Alexa-NA to A549 cells ($n = 2$).

AR, FCS binding studies on the A549 human lung cancer cell line were carried out which yielded a K_D of 5.98 ± 1.62 nM ($n = 2$) for Alexa-NA (Figure 3C) and a B_{max} of 15.10 ± 1.57 nM ($n = 2$). The receptor density (ρ) was calculated as 19.9 ± 2.0 μm^{-2} ($n = 5$). Similar to that of the hippocampal neurons, the maximum, noncorrelatable autofluorescence of the cell membranes was approximately 1.5 kHz (laser light energy of 14.2 kW/cm^2), and no binding of the pure dye was found, which made the A549 cells suitable for FCS experiments. Competitive binding between 5 nM Alexa-NA and 5 μM β_2-specific agonist terbutaline resulted in a level of nonspecific binding of 29%. A competition with the β_1/β_2-specific antagonist propranolol (5 μM) yielded a level of nonspecific binding of 23%, comparable to that of terbutaline, confirming the β_2-selective binding affinity of Alexa-NA for A549 cells. The binding rate constant (k_{on}) of 0.12 ± 0.02 s^{-1} nM^{-1} was on the same order of magnitude as that found for the hippocampal neurons (Figure 3D). The diffusion time constants for the receptor−ligand complexes [$\tau_{bound1} = 3.33 \pm 0.63$ ms ($n = 20$) and $\tau_{bound2} = 95.22 \pm 21.80$ ms ($n = 20$)] as well as the corresponding diffusion coefficients [$D_{bound1} = (2.88 \pm 1.72) \times 10^{-8}$ cm^2/s and $D_{bound2} = (1.01 \pm 0.46) \times 10^{-9}$ cm^2/s] were also comparable to the results obtained with the hippocampal neurons (Figure 6). In contrast, the maximum of 40% for the receptor−ligand complex with τ_{bound2} on the A549 cells was observed after 15−20 min (Figure 4B). In addition, internalization of the β_2-AR was investigated by scanning cells along the *z*-axis at various points in time. For quantification, the fluorescence intensity within the cytoplasm was integrated. The cell scans of a 10 nM Alexa-NA incubation yielded an intracellular fluorescence profile with a maximum value of 701 kHz μm ($n = 3$) after 20 min which confirmed the results obtained from the FCS binding studies (Figure 7). Co-incubation with 1 μM terbutaline increased the fluorescence intensity to 1311 kHz μm ($n = 3$) which then was observed within the next 40 min constantly. These observations were consistent with immunocytochemical patterns of subcellular receptor localization after treatment with terbutaline (Figure 8B). Moreover, preincubation with 1 μM forskolin, which leads to an increased level of receptor uptake due to stimulation of adenylate cyclase and enhanced phosphorylation of the β_2-AR by the phosphokinase GRK2 and subsequent internalization of the receptor, caused a drop in receptor density in the membrane which manifested itself in a decrease in the level of total binding from 50.3 ± 0.9 to 39.0 ± 1.0% following incubation with 7 nM Alexa-NA. The ratio of the receptor−ligand complex τ_{bound2} to the complex τ_{bound1} increased from 0.24 ± 0.03 to 0.32 ± 0.04 ($n = 3$), consistent with the notion that τ_{bound1} corresponds to the receptor which undergoes uptake.

Finally, an attempt was made to use FCS to discover agents which inhibit the receptor uptake process, because there is great therapeutic interest in manipulating G-protein-coupled receptor (GPCR) signal transduction (*20*). Besides the β_2-AR, certain components (e.g., GRK2, Src, etc.) involved in GPCR signal transduction are localized primarily in cholesterol-rich microdomains of the plasma membrane (*21*, *22*). Furthermore, alterations in local plasma membrane cholesterol content play a critical role in clathrin-coated pit

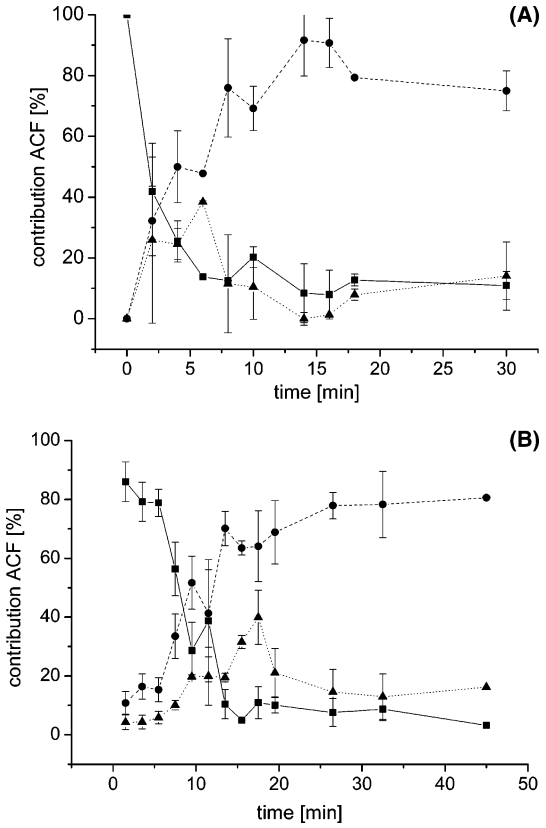

FIGURE 4: Time-dependent detection of the signal distribution to two different states of mobility of receptor−ligand complexes by incubation of 5 nM Alexa-NA with hippocampal neurons ($n = 2$) (A) and A549 cells ($n = 2$) (B): (■) freely diffusing Alexa-NA above the cell, (●) receptor−ligand complexes with free lateral mobility (τ_{bound1}), and (▲) receptor−ligand complexes with restricted lateral mobility (τ_{bound2}).

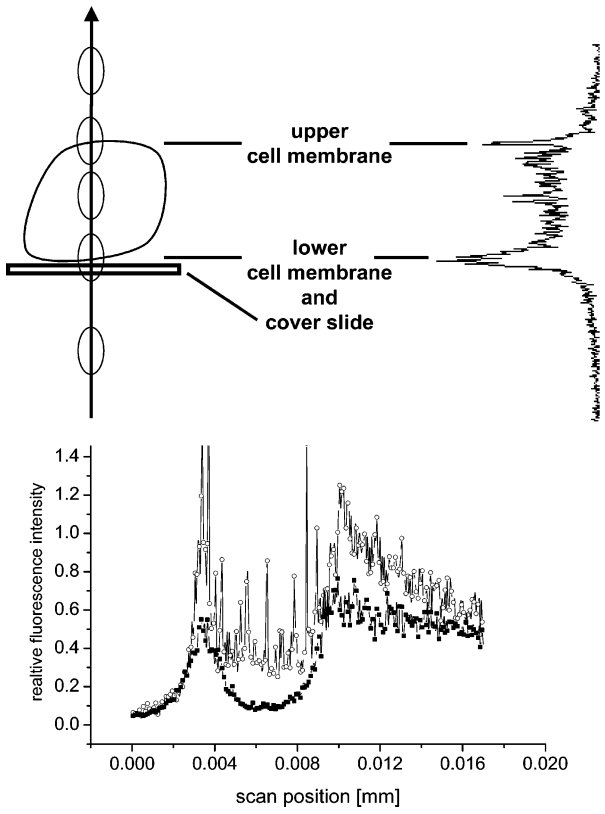

FIGURE 5: Cell scans in the *z*-direction through a hippocampal neuron initially (■) and after incubation for 5 min with 5.0 nM Alexa-NA (○). The appearance of membrane-associated and intracellular fluorescence events is time-dependent and refers to regulatory endocytotic processes, according to the distribution of the different diffusing receptor−ligand complexes, detected in FCS measurements (Figure 4).

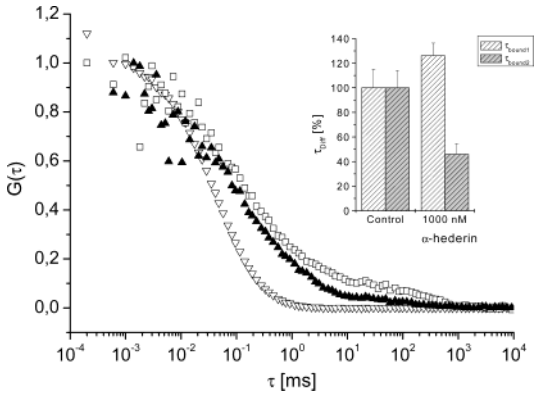

FIGURE 6: Normalized autocorrelation curves: (▽) freely diffusing Alexa-NA with a τ_{free} of 45.0 ± 0.41 μs ($n = 20$) above the cells, (□) Alexa-NA (4 nM) bound to the membrane of A549 cells with a τ_{bound1} of 3.33 ± 0.63 ms ($n = 20$) for the free lateral mobility of the receptor−ligand complex and a τ_{bound2} of 95.22 ± 21.80 ms ($n = 20$) for the hindered lateral mobility of the receptor−ligand complex, and (▲) preincubation with 1 μM α-hederin with a decrease in τ_{bound2} by 55% and an increase in τ_{bound1} by 26% ($n = 20$).

internalization (*23*−*25*). On the basis of the observation that cholesterol-complexing compounds termed saponins interfere with endocytosis, a screening of chemically defined saponins was performed (data not shown) (*26*, *27*). Among these compounds, pretreatment of A549 cells with 1 μM α-hederin (Figure 1) for 24 h inhibited the terbutaline-mediated increase in the level of β_2-AR uptake. After an incubation period of 20 min, a maximum inhibition of 87% ($n = 3$) was found (Figure 7).

From the analysis of the FCS autocorrelation curve, 1 μM α-hederin reduced the occurrence of the receptor−ligand complex with τ_{bound2} by 55 ± 1.8% ($n = 6$), whereas the occurrence of τ_{bound1} increased by 26 ± 0.7% ($n = 6$) (Figure 6). Additionally, α-hederin-treated A549 cells incubated with 4 nM Alexa-NA showed an increased level of ligand binding [from 55.2 ± 5.7 to 63.0 ± 3.2% ($n = 6$)].

The regulatory influence of α-hederin on receptor down-regulation was validated by immunocytochemical fluorescence detection of the β_2-AR via an anti-β_2 antibody. The untreated control showed weak punctate staining of the receptor, which could be related to clusters of the receptor occurring in the cell membrane and on vesicular structures in the cytoplasm (Figure 8A). Treatment with 10 μM the β_2-specific agonist terbutaline markedly increased the number and brightness of receptor aggregates (Figure 8B). From the FCS corresponding autocorrelation curves, the increase in the brightness of aggregates upon treatment with terbutaline was confirmed by an increase in the number of counts per molecule from 0.64 (the number of molecules of nontreated cells was 7.1 and the count rate 4.55 kHz) to 1.23 (the number of molecules was 3.6 and the count rate 4.59 kHz). A treatment with the antagonist propranolol (10 μM) significantly reduced the effect of a subsequent incubation with 10 μM terbutalin (Figure 8C). The preincubation with 1 μM α-hederin inhibited receptor aggregation and inter-

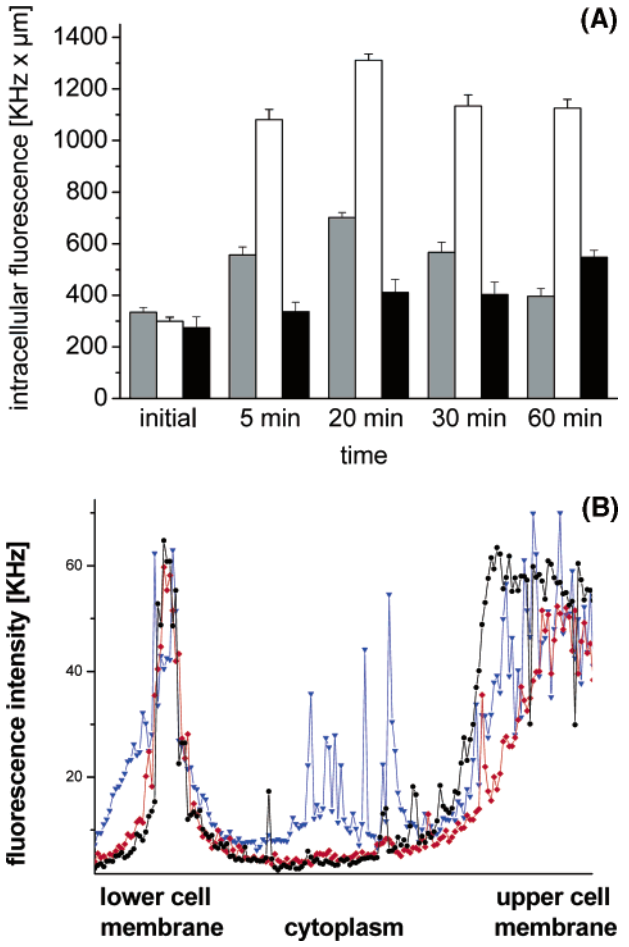

FIGURE 7: (A) Fluorescence intensity within the cytoplasm of A549 cells measured at various time points by cell scans in the z-direction using a sharply focused laser beam ($n = 3$): (gray bars) incubation with 10 nM Alexa-NA, (white bars) incubation with 10 nM Alexa-NA and 1 μM terbutaline, and (black bars) preincubation with 1 μM α-hederin for 24 h followed by an incubation with 10 nM Alexa-NA and 1 μM terbutaline. (B) Cell scan overlay after 20 min ($n = 3$): (●) incubation with 10 nM Alexa-NA, (▼) incubation with 10 nM Alexa-NA and 1 μM terbutaline, and (◆) preincubation with 1 μM α-hederin for 24 h and a second incubation with 10 nM Alexa-NA and 1 μM terbutaline.

nalization after a following incubation with 10 μM terbutaline, which is in good aggrement with both the results obtained from the FCS binding studies and the cell scans (Figure 8D).

DISCUSSION

The aim of this paper was to investigate dynamic processes of the β_2-adrenergic receptor (β_2-AR) on living cells following ligand binding, by means of FCS. For this purpose, arterenol was coupled with Alexa 532 and used for the studies as a fluorescently labeled ligand (Alexa-NA) with a specific binding affinity for the β_2-AR. The high photostability, high quantum yield, and good aqueous solubility of Alexa-NA are advantageous for FCS measurements on living cells because it is necessary, due to the expected autofluorescence, which is caused by the membrane components of the cell and the low concentration of ligands that are used in binding studies, to obtain a sufficiently high fluorescence signal through the labeled ligand (*28*). Incubation with 1 nM Alexa-NA and the hippocampal neurons resulted in a signal-to-background ratio of >10:1, which proved to be suitable for the measurements and disregarding the influence of the background signal.

Other specific ligands for the β_2-AR have also been coupled with fluorescence markers in the past. Heithier et al. labeled the β_1/β_2-specific antagonist CGP12177a with the dyes NBD, bodipy, and fluorescein and described the binding of those to cell preparations and intact cells with K_D values in the picomolar range (*29*, *30*). In 1982, Henis et al. synthesized NBD-labeled alprenolol (*31*), while the high level of nonspecific binding of this ligand to cell membrane preparations was described by Rademaker et al. (*32*). These publications showed, however, that it is possible to label small adrenergic ligands with relatively voluminous fluorescence markers and obtain a high binding affinity, although the binding pocket of the β-adrenergic receptors is located deep in the heptahelical bundle of the receptor protein (*33*−*35*).

Our labeling strategy took advantage of the dependence of the β-adrenergic ligand subtype selectivity on catecholamine substitution at the amine function to create a more β_2-specific ligand out of β_1-preferring arterenol. At this position, the succinimidyl ester-activated fluorescent dye was introduced via nucleophile substitution. On hippocampal neurons, Alexa-NA showed a 1000-fold higher affinity for β_2-AR than the underivatized structure. Consistently, a k_i value of 3.86 ± 0.28 μM for arterenol was measured at the β_2-AR of living cells, compared to the K_D value of 1.29 ± 0.31 nM of the fluorescent ligand. Competition experiments with the β_1/β_2-specific propranolol and the β_2-selective agonist terbutaline revealed comparable competition rates. This is proof of the β_2-selective binding of Alexa-NA to the β_2-AR (*28*, *29*).

When the K_D values of 1.29 ± 0.31 nM for the neurons and 5.98 ± 1.62 nM for the A549 cells are compared, high-affinity binding is seen to be present in both cases, with the difference therein possibly being the result of the differing compositions of the β-receptor populations. The hippocampal neurons have a lower content of β_2-receptors, in agreement with a low B_{max} (5.96 ± 0.27 nM), corresponding to a receptor density (ρ_N) of 4.5/μm^2 for the Alexa-NA binding and a calculated number of binding sites on the cell surface of approximately 2700 receptors/cell. Quantitative autoradiography of β_1- and β_2-adrenergic receptors in distinct hippocampus regions revealed β_1:β_2 ratios between 6.5:3.5 for CA3 (rostral) and 9:1 for CA1 (caudal) and different receptor levels of ∼22 and 76.5 fmol/mg of protein (*36*). The higher receptor density (ρ_{A549}) of 19.9 ± 2.0 μm^{-2} for the pulmonary cells in the preconfluent stage, which is equivalent to a total of approximately 12 000 receptors/cell, was also confirmed on this order of magnitude by Stern and Kunos (*38*).

In both cell models, the binding of Alexa-NA to the β_2-AR was seen in the course of the FCS experiments in three different diffusion coefficients. In addition to the free, unbound ligand with a D_{free} of (2.11 ± 0.04) × 10^{-6} cm^2/s, two distinct mobilities of receptor−ligand complexes were found. First, the complex with a diffusion coefficient (D_{bound1}) of (5.23 ± 0.64) × 10^{-8} cm^2/s at the neurons and (2.88 ± 1.72) × 10^{-8} cm^2/s at the A549 cells most likely corresponds to the lateral mobility of the receptor−ligand complex localized in caveolae of the cell membrane, because it was

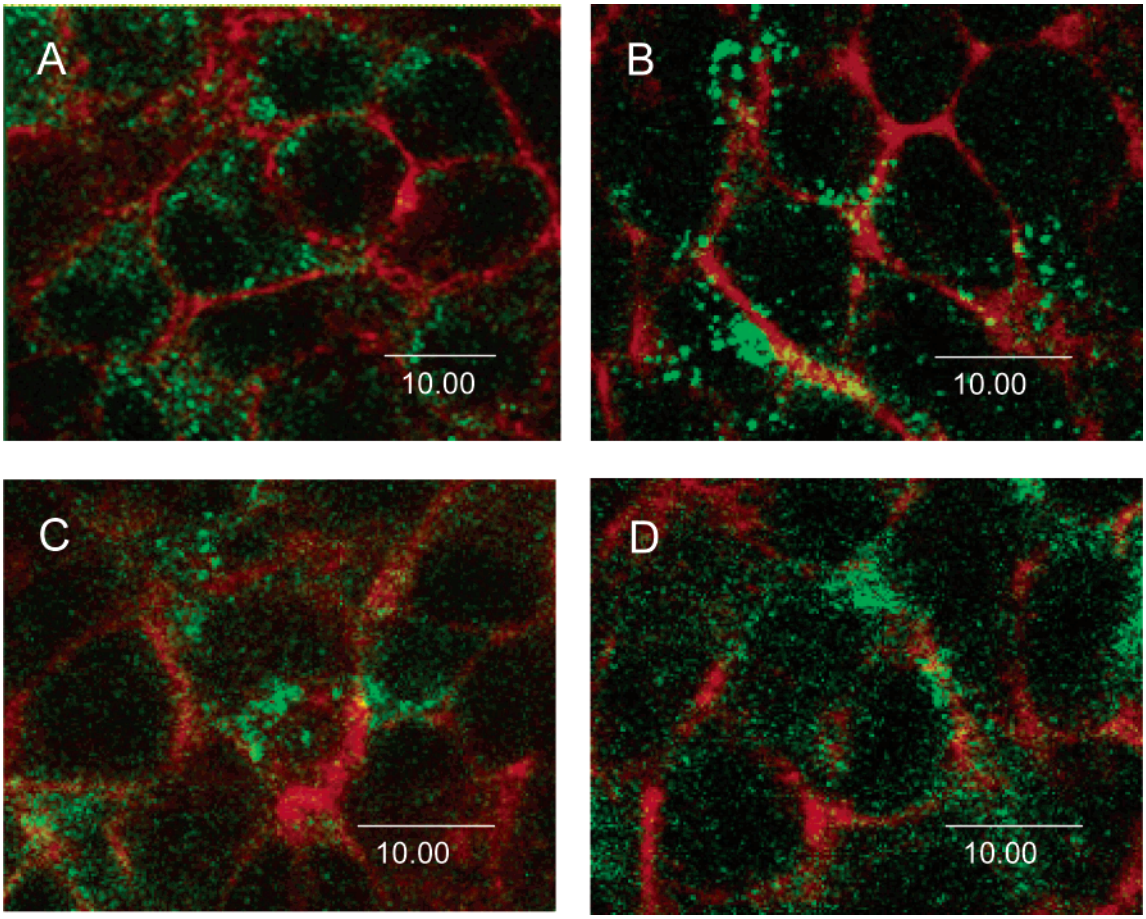

FIGURE 8: Confocal laser scanning images of the immunocytochemical detection of the β_2-AR (green fluorescence) on the A549 cells. Distribution of the β_2-AR on nonincubated cells (A), incubation with 10 μM terbutaline (B), preincubation with the antagonistic propranolol (10 μM), following incubation with 10 μM terbutaline (C), and preincubation with 1 μM α-hederin, following incubation with 10 μM terbutaline (D). Phalloidin was used as a counterstain to visulize the F actin cytoskeleton.

Table 1: Binding Parameters of Alexa-NA and Kinetic Data of Receptor−Ligand Complexes in Different Cell Types

	K_D (nM)	ρ_N (no. of receptors/μm^2)	D_{bound1} (cm^2/s)	D_{bound2} (cm^2/s)	K_{on} (s^{-1} nM^{-1})
hippocampal neurons	1.29 ± 0.31	4.5 ± 0.9	(5.23 ± 0.64) × 10^{-8}	(6.05 ± 0.23) × 10^{-10}	0.49 ± 0.03
A549 cells	5.98 ± 1.62	19.9 ± 2.0	(2.88 ± 1.72) × 10^{-8}	(1.01 ± 0.46) × 10^{-9}	0.12 ± 0.02

shown that resting β_2-ARs are found mainly in caveolae, e.g., in myocytes (*21*). In FRAP experiments, slower diffusion coefficients were found for the β_2-AR fused with green fluorescent protein (GFP) ($D = 4-12 \times 10^{-9}$ cm^2/s) (*39*) or occupied with an NBD-labeled agonist ($D = 1.4 \times 10^{-9}$ cm^2/s) (*31*), whereas caveolae, associated with GFP-tagged caveolin-1 fusion proteins, exhibited a diffusion coefficient (D) of 1.0×10^{-10} cm^2/s (*40*). However, the diffusion behavior of microdomains depends on the composition of the lipid bilayer and the size of the microdomain (*41*, *42*). Recently, in domain-forming giant unilamellar vesicles (GUVs), the key role of cholesterol in tuning the membrane lipid mobility was demonstrated (*25*). Native lipid rafts 50 nm in size diffuse faster ($D \sim 10^{-8}$ cm^2/s), whereas clustered microdomains, often bound to the cytoskeleton and physiologically observed to trigger signaling cascades, exhibit a hindered mobility (*43*).

The slower β_2-AR−Alexa-NA complex with a D_{bound2} of $(6.05 \pm 0.23) \times 10^{-10}$ cm^2/s (neurons) and a D_{bound2} of $(1.01 \pm 0.46) \times 10^{-9}$ cm^2/s (A549 cells) is clearly restricted in its mobility in the cell membrane. During incubation, the occurrence of receptor−ligand complexes with D_{bound2} is governed by a higher-order kinetic model and reached its maximum at the neuron membranes and A549 cells after ∼5 and ∼15−20 min, respectively. A similar restricted diffusion behavior on hippocampal neurons was found for the $GABA_A$ receptor ($D = 1.40 \times 10^{-9}$ cm^2/s) (*11*) and benzodiazepine receptor ($D = 2.63 \times 10^{-10}$ cm^2/s) after agonist binding (*7*). It is known that, following ligand binding, activated β_2-ARs move out of caveolae (*22*). These receptor−ligand complexes are then subject to regulation, which leads to endocytotic internalization via clathrin-coated pits, after a preliminary phosphorylation and subsequent binding to the adaptor proteins β-arrestin, dynamin, and AP-2 (*44*−*46*). Thus, we attribute the component with restricted mobility observed in FCS experiments to a receptor−ligand complex population, which, in the course of regulation after ligand binding, is subject to these processes. To confirm the attribution of the diffusion coefficients, co-incubation was performed with forskolin. Forskolin activates the adenylyl cyclase, which results in phosphorylation of the β_2-AR through GRK2 and consequently induces receptor internalization without previous ligand binding (*47*). Accordingly, the co-incubation of Alexa-NA with forskolin in the FCS

experiment demonstrated that the receptor population with free lateral mobility drops in the cell membrane and that the population of the receptor−ligand complex with hindered mobility, which is subject to regulatory processes, increases.

Internalization of the β_2-AR was furthermore confirmed by cell scans in the *z*-direction through A549 cells using 10 nM Alexa-NA alone and in a co-incubation with 1 μM terbutaline. In these experiments, the integrated fluorescence intensity of the cytoplasm increased by 87% in the presence of 1 μM terbutaline, which clearly demonstated the agonistic stimulation and internalization of the β_2-AR. Whereas the number of internalized receptors dropped after 20 min during the incubation of Alexa-NA with A549 cells, the co-incubation with terbutaline revealed a constantly high intracellular fluorescence intensity during the whole incubation period of 60 min. Obviously, the intense terbutaline stimulation prevented the receptor recycling process in terms of re-uptake of the β_2-AR into the cell membrane which subsequently leads to a decrease in the intracellular fluorescence intensity. Consistent with the notion that the low-mobility fraction of the β_2-AR corresponds to receptor molecules which undergo endocytosis, a preincubation for 24 h with the saponin compound α-hederin (1 μM) inhibited the terbutaline-stimulated internalization of the β_2-AR by 87% after 20 min, in agreement with the fact that saponins are cholesterol-complexing agents and that cholesterol depletion is known to inhibit receptor internalization (*23*−*26*).

Also in FCS experiments, α-hederin exhibited an inhibition of β_2-AR internalization in A549 cells. As a consequence, the level of binding of 4 nM Alexa-NA to A549 cells increased from 55.2 ± 5.7 to 63.0 ± 3.2%. The corresponding autocorrelation curve and the quantification of the different diffusion time constants revealed a decrease in the receptor−ligand complex τ_{bound2} by 55% and an increase in τ_{bound1} by 26%. Obviously, α-hederin led to a redistribution of receptor−ligand complexes with hindered mobility to receptor−ligand complexes with free lateral mobilty which may explain the inhibition of the regulatory processes after receptor occupation. Immunofluorescence studies confirmed this finding by a decreased occurrence of receptor aggregation within the cell membrane and a reduced number of clustered receptors as part of early endosomes after endocytosis. Although α-hederin did not show any affinity for the β_2-AR in FCS binding studies, a similar influence on the regulatory process analogues to the antagonistic propranolol was found in laser scanning microscope investigations.

With this work, different dynamics of β_2-adrenergic receptor−ligand complexes on living cells were described. Binding-dependent dynamics of receptor systems can be obtained simultaneously by FCS, which may lead to a better understanding of subcellular mechanisms of receptor regulation and signaling, especially under stimulating and inhibiting conditions.

ACKNOWLEDGMENT

We thank Dr. C. Culmsee for supplying the hippocampal neurons and Dr. G. Jaques for kindly providing the A549 cell line.

REFERENCES

1. Pierce, K. L., Premont, R. T., and Lefkowitz, R. J. (2002) Seven-transmembrane receptors, *Nat. Rev. Mol. Cell Biol. 3*, 639−650.
2. von Zastrow, M. (2001) Role of endocytosis in signalling and regulation of G-protein-coupled receptors, *Biochem. Soc. Trans. 29*, 500−504.
3. Carman, C. V., and Benovic, J. L. (1998) G-protein-coupled receptors: turn-ons and turn-offs, *Curr. Opin. Neurobiol. 8*, 335−344.
4. Barnes, P. J. (1995) β-Adrenergic receptors and their regulation, *Am. J. Respir. Crit. Care Med. 152*, 838−860.
5. Roth, B. L., Willins, D. L., and Kroeze, W. K. (1998) G protein-coupled receptor (GPCR) trafficking in the central nervous system: relevance for drugs of abuse, *Drug Alcohol Depend. 51*, 73−85.
6. Hadcock, J. R., and Malbon, C. C. (1988) Regulation of β-adrenergic receptors by "permissive" hormones: glucocorticoids increase steady-state levels of receptor mRNA, *Proc. Natl. Acad. Sci. U.S.A. 85*, 8415−8419.
7. Hegener, O., Jordan, R., and Häberlein, H. (2002) Benzodiazepine binding studies on living cells: application of small ligands for fluorescence correlation spectroscopy, *Biol. Chem. 383*, 1801−1807.
8. Magde, D., Elson, E. L., and Webb, W. W. (1972) Thermodynamic fluctuations in a reacting system: measurement by fluorescence correlation spectroscopy, *Phys. Rev. Lett. 29*, 705−708.
9. Magde, D., Elson, E. L., and Webb, W. W. (1974) Fluorescence correlation spectroscopy. II. An experimental realization, *Biopolymers 13*, 29−61.
10. Elson, E. L., and Madge, D. (1974) Fluorescence correlation spectroscopy. I. Conceptual basis and theory, *Biopolymers 13*, 1−27.
11. Meissner, O., and Häberlein, H. (2003) Lateral mobility and specific binding to $GABA_A$ receptors on hippocampal neurons monitored by fluorescence correlation spectroscopy, *Biochemistry 42*, 1667−1672.
12. Mattson, M. P., Cheng, B., Culwell, A. R., Esch, F. S., Lieberburg, I., and Rydel, R. E. (1993) Evidence for excitoprotective and intraneuronal calcium-regulating roles for secreted forms of the β-amyloid precursor protein, *Neuron 10*, 243−254.
13. Thompson, N. L. (1991) in *Topics in Fluorescence Spectroscopy* (Lakowicz, J. R., Ed.) Vol. 1, pp 337−378, Plenum Press, New York.
14. Starr, T. E., and Thompson, N. L. (2001) Total internal reflection with fluorescence correlation spectroscopy: Combined surface reaction and solution diffusion, *Biophys. J. 80*, 1575−1584.
15. Lieto, A. M., Cush, R. C., and Thompson, N. L. (2003) Ligand−receptor kinetics measured by total internal reflection with fluorescence correlation spectroscopy, *Biophys. J. 85*, 3294−3302.
16. Widengren, J., and Schwille, P. (2000) Characterization of photoinduced isomerization and back-isomerization of the cyanine dye Cy5 by fluorescence correlation spectroscopy, *J. Phys. Chem. A 104*, 6416−6428.
17. Rozanov, C. B., and Dratman, M. B. (1996) Immunohistochemical mapping of brain triiodothyronine reveals prominent localization in central noradrenergic systems, *Neuroscience 74*, 897−915.
18. Lathe, R. (2001) Hormones and the hippocampus, *J. Endocrinol. 169*, 205−231.
19. Liggett, S. B. (1999) Molecular and genetic basis of β2-adrenergic receptor function, *J. Allergy Clin. Immunol. 104*, S42−S46.
20. Lombardi, M. S., Kavelaars, A., and Heijnen, C. J. (2002) Role and modulation of G protein-coupled receptor signaling in inflammatory processes, *Crit. Rev. Immunol. 22*, 141−163.
21. Xiang, Y., Rybin, V. O., Steinberg, S. F., and Kobilka, B. (2002) Caveolar localization dictates physiologic signaling of β2-adrenoceptors in neonatal cardiac myocytes, *J. Biol. Chem. 277*, 34280−34286.
22. Rybin, V. O., Xu, X., Lisanti, P., and Steinberg, S. F. (2000) Differential targeting of β-adrenergic receptor subtypes and adenylyl cyclase to cardiomyocyte caveolae. A mechanism to functionally regulate the cAMP signaling pathway, *J. Biol. Chem. 275*, 41447−41457.
23. Subtil, A., Gaidarov, I., Kobylarz, K., Lampson, M. A., Keen, J. H., and McGraw, T. E. (1999) Acute cholesterol depletion inhibits clathrin-coated pit budding, *Proc. Natl. Acad. Sci. U.S.A. 96*, 6775−6780.
24. Rodal, S. K., Skretting, G., Garred, O., Vilhardt, F., van Deurs, B., and Sandvig, K. (1999) Extraction of cholesterol with methyl-β-cyclodextrin perturbs formation of clathrin-coated endocytic vesicles, *Mol. Biol. Cell 10*, 961−974.
25. Kahya, N., Scherfeld, D., Bacia, K., Poolman, B., and Schwille, P. (2003) Probing lipid mobility of raft-exhibiting model mem-

branes by fluorescence correlation spectroscopy, *J. Biol. Chem. 278*, 28109−28115.
26. Cerneus, D. P., Ueffing, E., Posthuma, G., Strous, G. J., and van der Ende, A. (1993) Detergent insolubility of alkaline phosphatase during biosynthetic transport and endocytosis. Role of cholesterol, *J. Biol. Chem. 268*, 3150−3155.
27. Caron, M. G., and Lefkowitz, R. J. (1976) Solubilization and characterization of the β-adrenergic receptor binding sites of frog erythrocytes, *J. Biol. Chem. 251*, 2374−2384.
28. Brock, R., Hink, M. A., and Jovin, T. M. (1998) Fluorescence correlation microscopy of cells in the presence of autofluorescence, *Biophys. J. 75*, 2547−2557.
29. Heithier, H., Jaeggi, K. A., Ward, L. D., Cantrill, R. C., and Helmreich, E. J. (1988) Synthesis and characterization of CGP-12177-NBD: a fluorescent β-adrenergic receptor probe, *Biochimie 70*, 687−694.
30. Heithier, H., Hallmann, D., Boege, F., Reilander, H., Dees, C., Jaeggi, K. A., Arndt-Jovin, D., Jovin, T. M., and Helmreich, E. J. (1994) Synthesis and properties of fluorescent β-adrenoceptor ligands, *Biochemistry 33*, 9126−9134.
31. Henis, Y. I., Hekman, M., Elson, E. L., and Helmreich, E. J. (1982) Lateral motion of β receptors in membranes of cultured liver cells, *Proc. Natl. Acad. Sci. U.S.A. 79*, 2907−2911.
32. Rademaker, B., Kramer, K., Stroes, J. W., Vlug, J., Krielaart, M., and Zaagsma, J. (1985) High affinity non-β-adrenoceptor binding of β-adrenergic ligands, *Eur. J. Pharmacol. 111*, 31−36.
33. Tota, M. R., and Strader, C. D. (1990) Characterization of the binding domain of the β-adrenergic receptor with the fluorescent antagonist carazolol. Evidence for a buried ligand binding site, *J. Biol. Chem. 265*, 16891−16897.
34. Cheung, A. H., Huang, R. R., and Strader, C. D. (1992) Involvement of specific hydrophobic, but not hydrophilic, amino acids in the third intracellular loop of the β-adrenergic receptor in the activation of Gs, *Mol. Pharmacol. 41*, 1061−1065.
35. Kobilka, B., Gether, U., Seifert, R., Lin, S., and Ghanouni, P. (1998) Examination of ligand-induced conformational changes in the β2 adrenergic receptor, *Life Sci. 62*, 1509−1512.
36. Rainbow, T. C., Parsons, B., and Wolfe, B. B. (1984) Quantitative autoradiography of β1- and β2-adrenergic receptors in rat brain, *Proc. Natl. Acad. Sci. U.S.A. 81*, 1585−1589.
37. Szentendrei, T., Lazar-Wesley, E., Nakane, T., Virmani, M., and Kunos, G. (1992) Selective regulation of β2-adrenergic receptor gene expression by interleukin-1 in cultured human lung tumor cells, *J. Cell. Physiol. 152*, 478−485.
38. Stern, L., and Kunos, G. (1988) Synergistic regulation of pulmonary β-adrenergic receptors by glucocorticoids and interleukin-1, *J. Biol. Chem. 263*, 15876−15879.
39. Barak, L. S., Ferguson, S. S. G., Zhang, J., Martenson, C., Meyer, T., and Caron, M. G. (1997) Internal trafficking and surface mobility of a functionally intact β2-adrenergic receptor-green fluorescent protein conjugate, *Mol. Pharmacol. 51*, 177−184.
40. Thomsen, P., Roepstorff, K., Stahlhut, M., and van Deurs, B. (2002) Caveolae are highly immobile plasma membrane microdomains, which are not involved in constitutive endocytic trafficking, *Mol. Biol. Cell 13*, 238−250.
41. Korlach, J., Schwille, P., Webb, W. W., and Feigenson, G. W. (1999) Characterization of lipid bilayer phases by confocal microscopy and fluorescence correlation spectroscopy, *Proc. Natl. Acad. Sci. U.S.A. 96*, 8461−8466.
42. Schütz, G. J., Kada, G., Pastushenko, V. P., and Schindler, H. (2000) Properties of lipid microdomains in a muscle cell membrane visualized by single molecule microscopy, *EMBO J. 19*, 892−901.
43. Simons, K., and Toomre, D. (2000) Lipid rafts and signal transduction, *Nat. Rev. Mol. Cell Biol. 1*, 31−39.
44. Ferguson, S. S. (2001) Evolving concepts in G protein-coupled receptor endocytosis: the role in receptor desensitization and signaling, *Pharmacol. Rev. 53*, 1−24.
45. Tsao, P., and von Zastrow, M. (2000) Downregulation of G protein-coupled receptors, *Curr. Opin. Neurobiol. 10*, 365−369.
46. Claing, A., Laporte, S. A., Caron, M. G., and Lefkowitz, R. J. (2002) Endocytosis of G protein-coupled receptors: roles of G protein-coupled receptor kinases and β-arrestin proteins, *Prog. Neurobiol. 66*, 61−79.
47. Post, S. R., Aguila-Buhain, O., and Insel, P. A. (1996) A key role for protein kinase A in homologous desensitization of the β2-adrenergic receptor pathway in S49 lymphoma cells, *J. Biol. Chem. 271*, 895−900.

BI035928T